Sound & Vibration

Tech Science Press

DOI: 10.32604/sv.2022.015634

ARTICLE

Dynamic Active Noise Control of Broadband Noise in Fighter Aircraft Pilot Helmet

Y. K. Bharath[1,*] and S. Veena[2]

[1]Malnad College of Engineering, Hassan, 573202, India

[2]National Aerospace Laboratories, Bengaluru, 560017, India

[*]Corresponding Author: Y. K. Bharath. Email: ykb@mcehassan.ac.in

Received: 01 January 2021 Accepted: 18 March 2021

ABSTRACT

This paper presents the development of a dynamic Active Noise Control (ANC) algorithm aimed towards reducing the broadband noise inside the helmet earcups of a fighter aircraft pilot helmet. The dynamic ANC involves a Variable Step-Size Griffiths (VSSG) FxLMS algorithm to attenuate noise entering directly through helmet, a LMS based adaptive noise canceller to attenuate noise entering through the pilot microphone, and energy detectors for failure protection and optimized battery power usage. The algorithms are implemented on Texas Instruments' TMS320C6748 processor and are tested in a helmet ANC experimental setup.

KEYWORDS

Active noise control; Variable Step-Size Griffiths algorithm; FxLMS

Nomenclature

$P(z)$	Primary path
$S(z)$	Secondary path
$\hat{S}_k(z)$	Secondary path estimate with M taps
$x(n)$	Reference input noise signal
$x'(n)$	Filtered input signal
$d(n)$	Earcup noise
$W_k(z)$	Main path filter with L taps
$y(n)$	Antinoise
$e(n)$	Residual noise at loudspeaker point
$e_e(n)$	Residual noise picked by error microphone
$\mu(n)$	Step-size
$P(n)$	Input signal power
β	Forgetting factor which decides cutoff frequency
G_k	Griffiths' cross-correlation coefficient
α	Step-size adaptation rate
σ	Residual noise tracker
$\nabla(n)$	Weight vector adaptation factor
Wnc_k	Noise canceller filter with L taps

$y_{nc}(n)$	Noise estimate of noise canceller
$e_{nc}(n)$	Noise free speech signal
eng_x	Energy of reference noise signal
eng_e	Energy of residual noise signal
R	ANC Resetting factor
f_s	Sampling frequency
B	Bandwidth

1 Introduction

The typical noise levels inside a fighter aircraft cockpit will be broadband and will be in the range from 95 to 105 dB. This level of noise exceeds the OSHA requirement of 85 dBA, 8 h/day exposure criterion, which may affect the alertness of the pilot and prolonged exposure may result in hearing impairment. Increased rate of periodontal diseases and cardiovascular risks in aircrew members because of high cockpit noise demands the reduction of noise levels [1–4]. Further, cockpit noise reaching the pilot's ear through radio communication channel affects the intelligibility of speech and makes the identification of caution signals difficult [5,6].

The primary objective of a pilot helmet is to provide safety. But, it also provides protection against certain amount of high frequency noise owing to passive noise attenuation achieved through its design and fitment [7]. However, considerable amount of low frequency noise will still penetrate the helmet and this can only be addressed with Active Noise Control (ANC) technique.

A few ANC headsets discussed in [8–16] perform satisfactorily in aircraft cabin environments and helicopters. But to address noise inside a fighter aircraft helmet, the ANC algorithm needs to be more specific and dynamic to handle high level of noise entering through multiple paths. The noise appearing in the helmet earcups is because of two components, one is the low frequency noise that enters through the helmet directly, referred to as Cockpit Noise Direct (CND) and the other one is the noise that enters through the pilot microphone via Audio Management Unit (AMU), denoted as Cockpit Noise through AMU (CNA). Currently existing Helmet ANC systems for fighter aircrafts focus only on CND [17–19]. In this paper CNA is also addressed along with CND.

Although tremendous efforts have been made by the scientific community to develop a better ANC system using machine learning algorithms like genetic algorithm, fuzzy logic, artificial neural network, etc. [20–25], the traditional adaptive algorithms have always proven to be more stable, computationally less intensive and quite attractive to be used in real-time applications. Generally, noises like CND is addressed using FxLMS based Feed Forward ANC (FFANC) algorithm [26]. But here, as the noise is broadband in nature, better tracking of ANC system is necessary with respect to the varying noise levels and characteristics of the aircraft noise. For this, various adaptive ANC algorithms are proposed [27–32]. In this paper, a Variable Step Size Griffiths (VSSG) algorithm for FxLMS algorithm as described in [33] has been used to achieve a faster convergence with lower residual noise. VSSG algorithms and its variants [34,35] have been proven for improved performance of LMS and FxLMS algorithms [36,37]. The second noise component, CNA is mitigated using an LMS based adaptive noise canceller.

In a typical ANC system, ANC algorithm starts execution once the system is powered ON, irrespective of the presence/absence of noise. This leads to unnecessary power consumption affecting the battery life. To tackle this, reference signal energy is used in this paper for turning ANC ON. Additionally, one of the major failure condition in the ANC system is the occurrence of divergence, which leads to the pilot being exposed to a higher level noise and deteriorated communication signals. This is a major safety issue and has to be addressed effectively. Signal energy [38,39] based tracking algorithm is proposed in this paper to address this issue. The algorithms proposed are targeted to meet the real-time requirements (majorly, less computational complexity and lower power consumption) of an embedded application. Further, the implementation of the algorithms is carried out on a Texas Instruments TMS320C6748 floating point DSP processor and its performance is demonstrated in a helmet ANC experimental setup.

2 Dynamic ANC Algorithms

Fig. 1 shows the block diagram schematic of helmet ANC system. As discussed, the two noise components, CND and CNA are addressed using FFANC and adaptive noise canceller respectively. The cockpit noise picked up by reference microphone is used as noise reference $x(n)$ for both FFANC and adaptive noise canceller. FFANC is based on VSSG FxLMS algorithm and has two separate channels for each earcup. The generated antinoise is fed through the audio communication speakers present inside the earcups. Adaptive noise canceller is based on LMS and its output (filtered pilot microphone signal) is fed to the same speakers. The residual noise is captured using error microphones placed inside the earcups. The algorithms to facilitate the dynamic operation of ANC so as to handle the scenarios in aircraft noise are depicted in Fig. 2 and are discussed in following subsections.

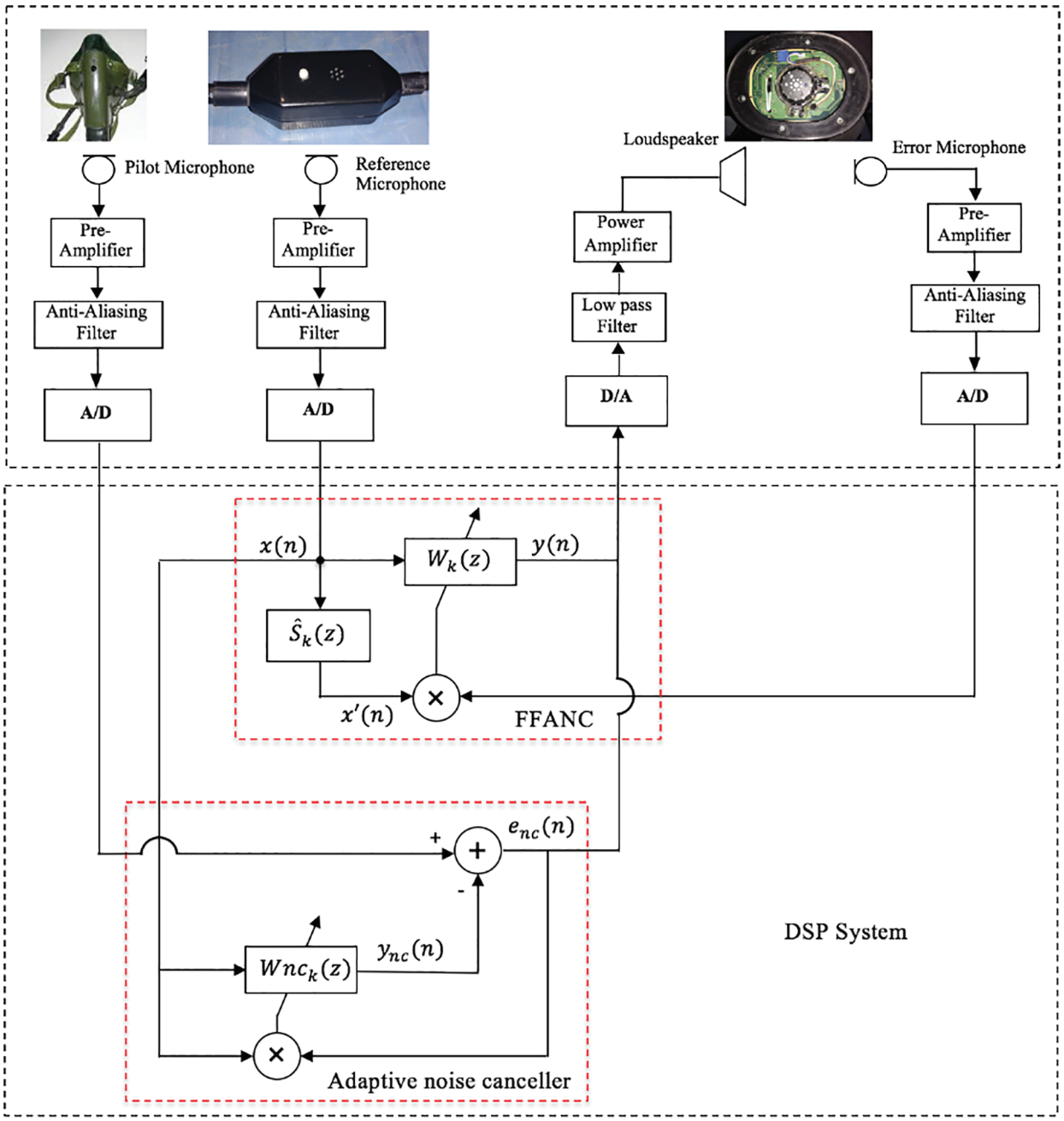

Figure 1: Block diagram schematic of Helmet ANC system

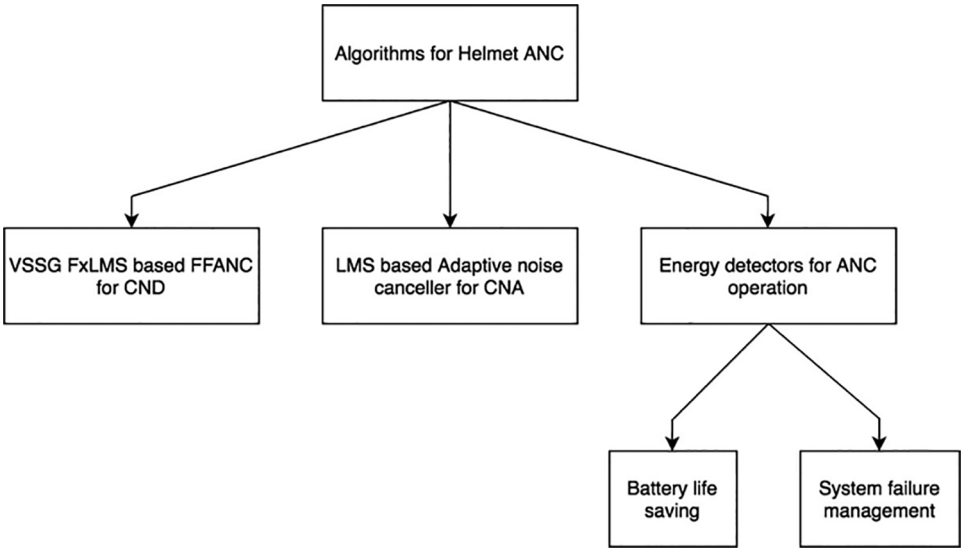

Figure 2: Algorithms for Helmet ANC

2.1 VSSG FxLMS Algorithm for CND

In Normalized FxLMS algorithm as shown in Fig. 3, proposed by Sen et al. [26], the transfer function path between the reference microphone and the speaker is referred to as primary path denoted by $P(z)$. The path between speaker and error microphone is referred to as secondary path denoted by $S(z)$, which is normally estimated offline (with random noise additive technique using LMS algorithm). $x(n)$ is the noise picked up by the reference microphone and $d(n)$ is the noise inside the earcup.

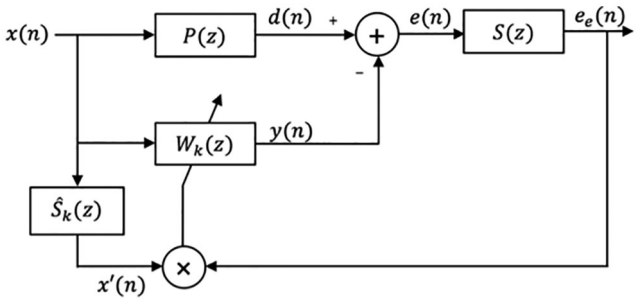

Figure 3: FFANC using FxLMS algorithm

To estimate $P(z)$, an adaptive FIR filter $W_k(z)$ having L number of taps is used. Its coefficients are adjusted using,

$$W_k(n+1) = W_k(n) + \mu'(n) e_e(n)\, x'(n-k); \qquad k = 0,\ 1,\ \ldots L-1 \tag{1}$$

where,

$W_k(n)$-main path filter.

$e(n)$-residual noise at the loudspeaker point.

$e_e(n)$-residual noise picked by error microphone.

In FxLMS algorithm, the input $x(n)$ is filtered using the secondary path estimate $\hat{S}_k(z)$ having M number of taps, given by,

$$x'(n) = \sum_{k=0}^{M-1} \hat{S}_k(n)\, x(n-k) \tag{2}$$

To compensate the large fluctuations in power levels of $x(n)$, the step size is normalized using,

$$\mu'(n+1) = \frac{\mu(n)}{(L+M)\, P(n+1)} \tag{3}$$

$$P(n+1) = \beta_n P(n) + (1-\beta_n)\, x'(n)^2 \tag{4}$$

$P(n)$ is the signal power. $0 < \beta_n < 1$ is known as the forgetting factor and should be small for fast varying signals.

Finally, the antinoise is computed using,

$$y(n) = \sum_{k=0}^{L-1} W_k(n) x(n-k) \tag{5}$$

This signal is fed to the speakers to cancel the acoustic noise. In LMS/FxLMS ANC algorithms, the convergence speed and final residual noise level depends on the step size μ. Large values of μ gives faster convergence but with higher residual noise. Smaller values of μ results in lower residual noise but with slower convergence. However, ANC is expected to have better tracking, i.e., to have faster convergence with least residual noise possible. With a fixed μ, any one of the objective is achievable. To have both advantages, Variable Step-Size Griffiths (VSSG) algorithm for FxLMS algorithm proposed by Narasimhan et al. [33] is used. This allows to have a larger step size in the beginning and a smaller step-size towards the convergence.

This algorithm is based on Griffiths' cross correlation coefficient between reference noise $x'(n)$ and error $e_e(n)$ and is estimated by,

$$G_k(n+1) = \beta_{vs} G_k(n) + (1-\beta_{vs})\, d(n)\, x'(n-k); \qquad k = 0,\ 1,\ \ldots L-1 \tag{6}$$

The step-size is updated using,

$$\mu(n+1) = \alpha\, \mu(n) + \sigma \sum_{k=0}^{L-1} [G_k(n) - y(n)\, x'(n-k)]^2 \tag{7}$$

A higher value of σ enables the step-size to track the changes in the residual noise at a faster rate for non-stationary signals. β_{vs} determines the cutoff frequency. Therefore, the new adaptation rule for the weight coefficients of FxLMS algorithm is given by,

$$W_k(n+1) = W_k(n) + \mu(n)\nabla(n), \qquad k = 0,\ 1,\ \ldots L-1 \tag{8}$$

Here, the weight vector adaptation gradient $\nabla(n)$ is computed using,

$$\nabla(n) = \frac{1}{(L+M)P(n)} \sum_{k=0}^{L-1} [G_k(n) - y(n)x'(n-k)] \tag{9}$$

The noise free Griffiths' cross correlation term $G_k(n)$ used for computing gradient $\nabla(n)$. The step-size $\mu(n)$ adaptation by VSSG FxLMS algorithm significantly enhances the convergence characteristics.

2.2 Adaptive Noise Canceller for CNA

To address CNA, a LMS based adaptive noise canceller is used. The signal coming from Audio Management Unit (AMU) constitutes of ATC communication signals, warning signals, pilot speech and CNA. With the use of this adaptive noise canceller, CNA alone can be addressed without affecting other signals.

As shown in Fig. 4, the path between reference mic and pilot mic, denoted as $Q(z)$, is identified using LMS algorithm. The weight updation of adaptive filter $Wnc_k(z)$ having L number of taps is done using,

$$Wnc_k(n+1) = Wnc_k(n) + \mu'_{nc}(n)\, e_{nc}\, x(n-k); \qquad k = 0,\ 1,\ \ldots L-1 \tag{10}$$

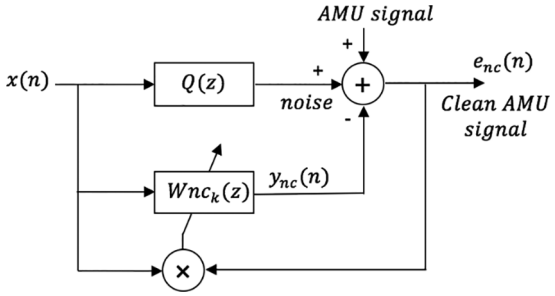

Figure 4: Adaptive noise canceller based on LMS algorithm

The step size is normalized using,

$$\mu'_{nc}(n+1) = \frac{\mu_{nc}(n)}{L\, P_{nc}(n+1)} \tag{11}$$

$$P_{nc}(n+1) = \beta_{nc} P_{nc}(n) + (1-\beta_{nc})\, x(n)^2 \tag{12}$$

Here, P_{nc} is the signal power. To remove the noise form noisy AMU signal, the noise signal estimate $y_{nc}(n)$ is computed by,

$$y_{nc}(n) = \sum_{k=0}^{N-1} Wnc_k(n)\, x(n-k) \tag{13}$$

$$e_{nc}(n) = (noise + AMU\ signal) - y_{nc}(n) \tag{14}$$

The noise free AMU signal $e_{nc}(n)$ is an electrical signal, which is added to FFANC antinoise signals and fed to the speakers.

2.3 Energy Based Detectors for ANC Operation

To achieve battery efficiency, ANC unit has to be turned ON only when the engine starts running. To achieve this, an energy based detector is employed where the Short Term Energy (STE) of $x(n)$ is used to determine the presence and absence of noise inside the cockpit.

For this, the energy of reference noise $x(n)$ is continuously computed using,

$$eng_x = \frac{1}{N} \sum_{i=0}^{N-1} x(n)^2 \tag{15}$$

where, N is the length of the circular buffer typically in the order of 1024.

The ANC unit is turned ON only if eng_x crosses a threshold. If eng_x goes below threshold, ANC unit is turned OFF. The threshold value is set based on the minimum signal power when engine is turned ON.

In any aircraft management application, detecting the condition of failure and its management is a major task. In the case of helmet ANC, the increase of noise inside the earcups due to divergence of ANC algorithm is considered as the major failure condition as this results in increased amount of noise and affects the intelligibility of communication signals. This is a catastrophic condition and has to be handled effectively by resetting ANC by cautiously detecting divergence.

For this, the ANC RESET factor R is computed as the gain in decibels,

$$R = 20\ log_{10}\left(\frac{eng_e}{eng_x}\right) \tag{16}$$

where,

$$eng_e = \frac{1}{N}\sum_{i=0}^{N-1} e_e(n)^2 \tag{17}$$

If R crosses the 3 dB margin during ANC operation, the ANC RESET condition is invoked by resetting W_k and all related buffers.

3 Simulation Results

For simulation of ANC algorithms, the cockpit noise of a Light Combat Aircraft (LCA) was recorded using M-Audio digital noise recorder. The recorded data consist of temporal noise during the takeoff, flight and landing conditions. The noise levels were recorded using a B&K 2270 sound level meter, which showed that the noise levels vary between 90 dBA–110 dBA. From the periodogram computed using MATLAB and one third octave spectrum computed using DATS analysis tool indicated that the noise spectrum was of broadband nature with significant contribution from low frequency components.

The algorithms discussed in Section 2 are simulated in MATLAB with parameters given in Table 1. A practical impulse response of length 128 samples is used for VSSG-FXLMS and adaptive noise canceller. The comparison of ANC with and without VSSG can be seen in Fig. 5.

Table 1: Parameters used for ANC simulation

Parameter	μ	μ_{max}	μ_{min}	β_n	β_v	α	σ	μ_{nc}	β_{nc}
Value	0.1	1	0.02	0.999	0.999	0.0001	0.99	0.1	0.999

In Table 1, μ is the step size for ANC without VSSG. In ANC with VSSG, initially the step size is μ_{max}. Towards convergence, the step size keeps on decreasing and is stagnated to μ_{min} to stop further reduction. In Fig. 5, improved performance of ANC using VSSG-FXLMS can be observed with respect to convergence time and residual error.

A speech signal corrupted by fighter aircraft noise is considered for simulation of adaptive noise canceller. Fig. 6 shows the convergence of adaptive noise canceller.

Fig. 7 shows the simulation of algorithms for battery saving and system failure management, which are included to control ANC algorithm. It can bee observed that whenever ANC diverges, the main path filter coefficients are reset and antinoise starts to build from initial conditions. It can be seen that as the power of the reference signal varies, ANC system stabilizes itself on its own.

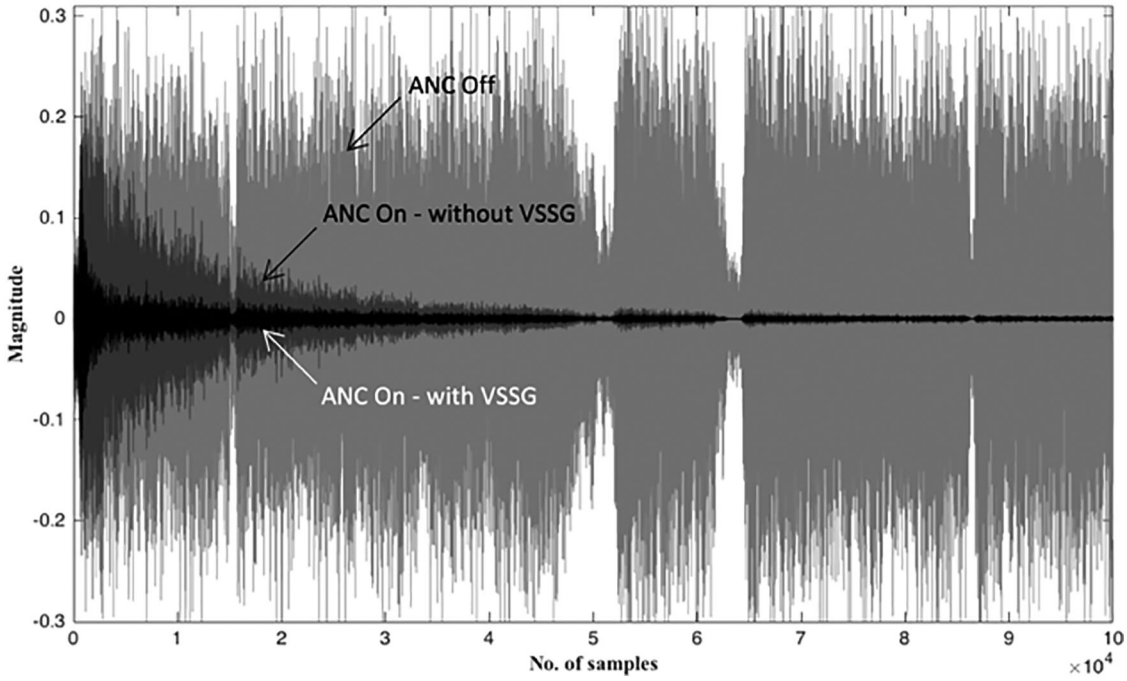

Figure 5: Comparison of ANC with and without VSSG

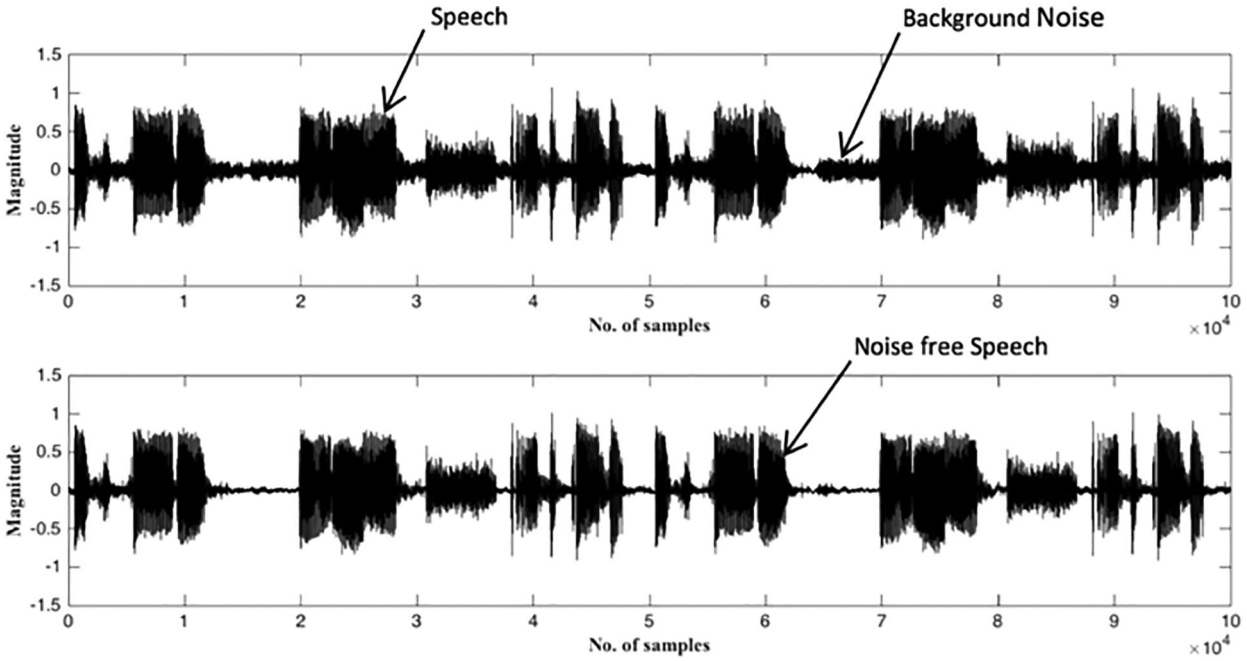

Figure 6: Convergence of adaptive noise remover

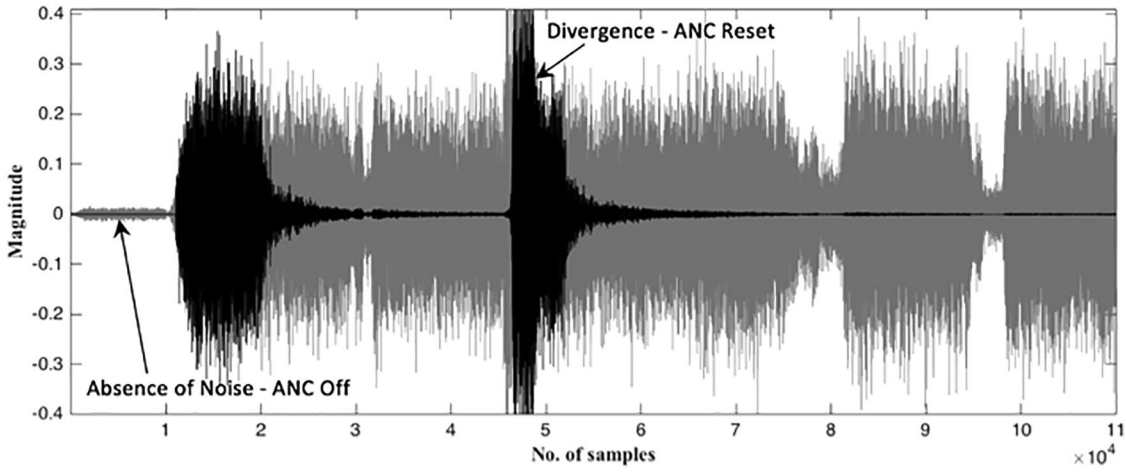

Figure 7: ANC response with absence of noise and occurrence of divergence

4 Causality Condition for ANC Operation

For effective noise cancellation, antinoise must be available by the time the noise signal arrives at the speaker. It implies that the acoustical delay must be greater than the electrical delay. This is referred to as causality condition. This is a time constraint imposed by the ANC system and the real-time implementation of ANC algorithms must adhere to this condition. Fig. 8 depicts the delays involved in both acoustic and electrical domain.

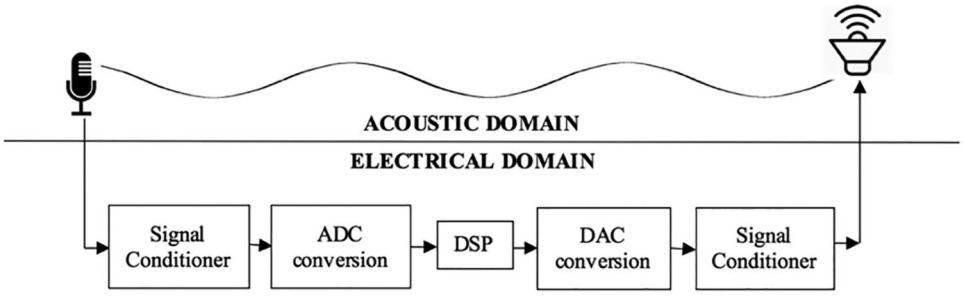

Figure 8: ANC casualty condition

The acoustic delay from the input microphone to the speaker is given as,

$$A = \frac{L}{C_0} \tag{18}$$

where,

A–Acoustical delay.

L–Distance between reference microphone and speaker in meters.

C_0–Speed of sound in air in m/s.

Electrical delay is due to the delay involved in antinoise generation. The delay path involves the electronics and DSP processor. Apart from the application loop time of DSP, the lowpass filters contribute significantly to the electrical delay.

In case of helmet ANC, for typical distance of 20 cm between reference microphones to speaker, the causality condition states that the DSP should operate at 14 kHz, for 8^{th} order butterworth filter [26]. To facilitate this condition, the algorithms have to be coded using processor specific assembly language only.

5 Real Time Evaluation of Dynamic ANC System

As shown in Fig. 1, the reference noise from the cockpit is picked up using a high performance electret microphone. Microphones are fitted inside the helmet earcups for fetching error signals. The communication speakers fitted inside the earcups are used for ANC system as well. The ANC unit consists of a low power high performance DSP board based on TMS320C6748 and a signal conditioner board which consists of pre amplifiers for microphones, low pass filters, A/D and D/A converters, anti-aliasing filters, reconstruction filters and power amplifier for loud speakers. It also has an SD card slot for recording the residual noise inside the helmet earcup (error microphone signal) for offline analysis of ANC performance. The ANC unit is powered by a 9 V rechargable battery. The AMU simulator mixes the pilot microphone signal with the communication signals received from Air Traffic Control (ATC).

To meet the computational requirements of the algorithms, they are coded with pre-estimated secondary path coefficients on DSP processor using processor specific hand optimized assembly language coding. With optimized coding, s sampling frequency of 14 kHz was achieved which greatly increases the processing speed of the DSP. The operating noise frequency range of ANC is largely affected by the the execution speed of ANC algorithm on the DSP board. As the Nyquist sampling criteria suggests: to avoid aliasing, the operation bandwidth should always be less than half of the sampling frequency, i.e., $B < f_s/2$ [40]. Hence the ANC cutoff frequency was set to 4 kHz (i.e., ANC will satisfactorily operate to the noise components having frequencies upto 4 kHz).

The experiments were conducted in an acoustically treated semi-anechoic chamber at CSIR-NAL (Fig. 9). Recorded cockpit noise is played using a 100W loudspeaker and the audio signals from error microphones are recorded in the SD card during ANC is Off and On.

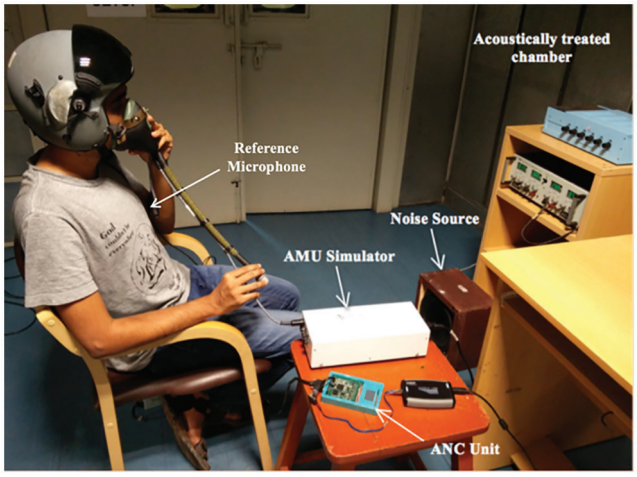

Figure 9: Experimental setup for testing helmet ANC system

The Power Spectral Density (PSD) of the cockpit reference noise, residual noise signals during ANC is Off and On are computed. The Noise attenuation in terms of decibels at particular frequencies is shown in Fig. 10. It can be observed from Fig. 10 that the helmet filters out much of the high frequency noise components of cockpit noise (passive noise attenuation) and the ANC unit effectively handles low frequency noise components within 4 kHz.

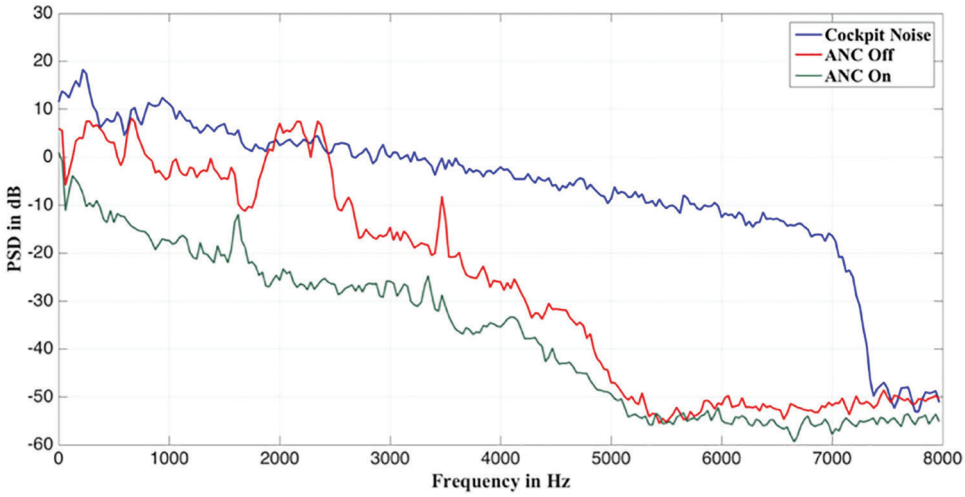

Figure 10: Dynamic ANC system performance in frequency domain

The ANC system performance is normally defined as the attenuation achieved in terms of Signal to Noise Ratio (SNR) in dB, which is computed using,

$$SNR = 10\ log_{10}\ \sum_{n=1}^{N} e_e^{ANC\ On}(n)^2 / \sum_{n=1}^{N} e_e^{ANC\ Off}(n)^2 \tag{19}$$

The passive and active noise attenuation achieved by the Helmet and dynamic ANC respectively are tabulated in Table 2.

Table 2: Performance of dynamic helmet ANC

	Passive noise attenuation achieved by the helmet without ANC compared to noise outside the helmet	Noise attenuation achieved by dynamic ANC compared to noise inside the helmet without ANC
Attenuation achieved	26 dB	18.06 dB

The ANC helmets and headsets discussed in [8–16], give passive noise attenuation of 10–15 dB and active noise reduction of 5–10 dB. Compared to these, the proposed dynamic ANC system gives passive noise reduction of 26 dB and active noise attenuation of 18.06 dB as seen from Table 2.

6 Conclusion

In this paper, a dynamic ANC system has been presented which proves suitable for a fighter aircraft pilot helmet. The ANC unit caters the noise entering through helmet using FFANC. The noise entering through AMU is catered using adaptive noise canceller. The robustness of the system was increased by using VSSG FxLMS algorithm which facilitates faster convergence and lower residual noise. Energy based detectors used for ANC operation control saves battery charge life cycle. The processor specific assembly language used for coding algorithms facilitated higher sampling rate enabling the generation of more samples of antinoise per second. The real-time evaluation shows that the dynamic helmet ANC system is capable of attenuating significant amount fighter aircraft cockpit noise.

Acknowledgement: Authors acknowledge National Aerospace Laboratories, Bangalore for ANC laboratory setup where the experiments were carried out.

Funding Statement: The project was funded by National Programme on Micro and Smart Systems (NPMaSS), Aeronautical Development Agency (ADA), Bangalore. Grant No. ADA/NPMASS159/2015, S. Veena, https://ada.gov.in/.

Conflicts of Interest: The authors declare that they have no conflicts of interest to report regarding the present study.

References

1. Gasaway, D. C. (1989). Noise levels in cockpits of aircraft during normal cruise and considerations of auditory risk. In: *Aviation, space, and environmental medicine*. USA: National Library of Medicine.
2. Thomas, M., Frank, P. S., Sabastian, S., Johannes, H., Andreas, D. et al. (2018). Environmental noise and cardiovascular system. *Journal of the American College of Cardiology, 71(6),* 688–697. https://doi.org/10.1016/j.jacc.2017.12.015
3. Landstrm, U., Lfstedt, P. (1987). Noise, vibration and changes in wakefulness during helicopter flight. In: *Aviation, space, and environmental medicine*. USA: National Library of Medicine.
4. Berglund, B., Lindvall, T., Schwela, D. H. (2002). Guideines for community noise. In: *Executive summary*. USA: World Health Organization.
5. Wagstaff, A. S., Woxen, O. J. (2001). Double hearing protection and speech intelligibility-room for improvement. In: *Aviation, space, and environmental medicine*. USA: National Library of Medicine.
6. Nixon, C., Morris, L. J., McCavitt, A. R., McKinley, R. L., Anderson, T. R. et al. (1998). Female voice communications in high level aircraft cockpit noises—part II: Vocoder and automatic speech recognition systems. In: *Aviation, space, and environmental medicine*. USA: National Library of Medicine.
7. Hmlinen, O. (1993). Flight helmet weight, +Gz forces, and neck muscle strain. In: *Aviation, space, and environmental medicine*. USA: National Library of Medicine.
8. Aviation Headsets Bose. https://www.bose.com/enus/products/headphones/aviationheadsets.html
9. Gentex aircrew rotary wing helmet systems. https://www.gentexcorp.com/gentex/defense/air/aircrew-rotary-wing-helmet-systems/
10. Woon, S. G., Sohini, M., Sen, M. K. (2005). Adaptive feedback active noise control headset: Implementation, evaluation and Its extensions. *IEEE Transactions on Consumer Electronics, 51(3),* 975–982. https://doi.org/10.1109/TCE.2005.1510511
11. Bhan, L., Woon-Seng, G., DongYuan, S., Masaharu, N., Stephen, E. (2021). Ten questions concerning active noise control in the built environment, building and environment. *Building and Environment, 200,* 1–18.
12. Charles, H. B., Micheal, S. G. (2011). Motorcycle helmet noise and active noise reduction. *The Open Acoustics Journal, 411(1),* 14–24.
13. Rosa, C., Ricardo, S. S. (2010). Active noise hybrid time-varying control for motor cycle helmets. *IEEE Transactions on Control Systems Technology, 18(3),* 602–612. https://doi.org/10.1109/TCST.87
14. Kuo, S. M., Chen, Y. R., Chang, C. Y., Lai, C. W. (2018). Development and evaluation of light-weight active noise cancellation earphones. *Applied Sciences, 8(7),* 1178.
15. Chang, C. Y., Chuang, C. T., Kuo, S. M., Lin, C. H. (2022). Multi-functional active noise control system on headrest of airplane seat. *Mechanical Systems and Signal Processing, 167(1),* 108552.
16. Zequiang, Z., Ming, W., Lan, Y., Chen, G., Jun, Y. et al. (2022). Robust parallel virtual sensing method for feedback active noise control in a headrest. *Mechanical Systems and Signal Processing, 178,* 1–24.
17. Colin, H. H. (2005). Current and future industrial applications of active noise controller. *Noise Control Engineering Journal, 53(5),* 1–35.
18. Pentti, K. (2004). *Military aviation noise-noise-induced hearing impairment and noise protection*. Finland: Oulu University Press.

19. Pääkkönen, R., Kuronen, P., Korteoja, M. (2001). Active noise reduction in aviation helmets during a military jet trainer test flight. *Scandinavian Audiology, Supplement, 52,* 177–179.
20. Chang, C. Y., Chen, D. R. (2010). Active noise cancellation without secondary path identification by using an adaptive genetic algorithm. *IEEE Transactions on Instrumentation and Measurement, 59(9),* 2315–2327. https://doi.org/10.1109/TIM.2009.2036410
21. Lu, L., Zhu, G., Yang, X., Zhou, K. (2022). Conjugate gradient-based FLANN algorithms in nonlinear active noise control. *Journal of the Franklin Institute, 359(9),* 4468–4488. https://doi.org/10.1016/j.jfranklin.2022.04.002
22. Guo, H., Wang, Y. S., Yang, C., Wang, X. L., Liu, N. N. (2019). Vehicle interior noise active control based on piezoelectric ceramic materials and improved fuzzy control algorithm. *Applied Acoustics, 150,* 216–226. https://doi.org/10.1016/j.apacoust.2019.02.018
23. Nirmal, K. R., Debi, P. D., Ganapati, P. (2019). PSO based narrowband ANC algorithm without the use of synchronization signal and secondary path estimate. *Mechanical Systems and Signal Processing, 114,* 378–398. https://doi.org/10.1016/j.ymssp.2018.05.018
24. Zhang, H., Wang, D. (2021). Deep ANC: A deep learning approach to active noise control. *Neural Networks, 141,* 1–10. https://doi.org/10.1016/j.neunet.2021.03.037
25. Zhou, Y. L., Zhang, Q. Z., Li, X. D., Gan, W. S. (2005). Analysis and DSP implementation of an ANC system using a filtered error neural network. *Journal of Sound and Vibration, 285(1),* 1–25.
26. Sen, M. K., Morgan, D. R. (1995). *Active noise control systems, algorithms and dsp implementations*. USA: Wiley.
27. Yao, J., Shuming, C., Hao, M., Zhengdao, Z., Wei, L. (2021). A novel adaptive step-size hybrid active noise control system. *Applied Accoustics, 182,* 1–14.
28. Jiang, J., Li, Y. (2018). Review of active noise control techniques with emphasis on sound quality enhancement. *Applied Accoustics, 136,* 139–148. https://doi.org/10.1016/j.apacoust.2018.02.021
29. Özge, C. U., Hatice, D. (2021). Speech protected noise cancellation system in noise dominated environments. *Applied Accoustics, 189,* 1–10.
30. Yang, D. P., Song, D. F., Zeng, X. H., Wang, X. L., Xhang, X. M. (2022). Adaptive nonlinear ANC system based on time-domain signal reconstruction technology. *Mechanical Systems and Signal Processing, 162,* 1–18. https://doi.org/10.1016/j.ymssp.2021.108056
31. Shi, D., Gan, W. S., Lam, B., Shen, X. (2021). Comb-partitioned frequency-domain constraint adaptive algorithm for active noise control. *Signal Processing, 188,* 1–13.
32. Muhammed, T. A. (2019). A time-varying normalized step-size based generalized fractional moment adaptive algorithm and its application to ANC of impulsive sources. *Applied Accoustics, 155,* 240–249. https://doi.org/10.1016/j.apacoust.2019.05.030
33. Narasimhan, S. V., Veena, S., Lokesha, H. (2009). Variable step-size Griffiths' algorithm for improved performance of feed forward/feedback active noise control. *Signal, Image Processing, 4(3),* 309–317.
34. Roopa, S., Narasimhan, S. V. (2014). Transform domain Variable Step-Size Griffiths Least Mean Square adaptive algorithm and its applications. *Computers and Electrical Engineering, 40(4),* 1028–1041. https://doi.org/10.1016/j.compeleceng.2013.11.025
35. Roopa, S., Narasimhan, S. V. (2017). Improved DCT domain variable step-size Griffith's LMS algorithm based active noise control using observation noise cancellers for secondary path identification. *International Journal of Vehicle Noise and Vibration, 13(2),* 118–136. https://doi.org/10.1504/IJVNV.2017.087907
36. Jing, C., Jun, Y. (2022). A distributed FxLMS algorithm for narrowband active noise control and its convergence analysis. *Journal of Sound and Vibration, 532,* 1–17.
37. Gong, C., Wu, M., Guo, J., Chen, J., Zhang, Z. et al. (2022). Statistical analysis of multichannel FxLMS algorithm for narrow band active noise control. *Signal Processing, 200,* 1–18.
38. Simon, H., Barry, V. V. (2002). *Signals and systems*. USA: Wiley.
39. Simon, H. (1996). *Adaptive filter theory.* Canada: Prentice-Hall.
40. Harry, N. (1928). Certain topics in telegraph transmission theory. *Transactions of the American Institute of Electrical Engineers, 47(2),* 617–644. https://doi.org/10.1109/T-AIEE.1928.5055024